



*Research article*

## **Thermal magnetic analysis on iron ores and banded iron formations (BIFs) in the Hamersley Province: Implications of origins of magnetic minerals and iron ores**

**William Guo\***

School of Engineering and Technology, Central Queensland University, North Rockhampton QLD 4702, Australia

\* **Correspondence:** Email: [w.guo@cqu.edu.au](mailto:w.guo@cqu.edu.au); Tel: 61749309687.

**Abstract:** The genesis models of the iron-ores hosted in banded iron formations (BIFs) in the Hamersley Province of Western Australia have been debated since the iron-ore deposits were discovered in the 1960s. The existing models considered the few physicochemical conditions for the iron-ore enrichment from BIFs. This study incorporates the latest research outcomes in conversions among the major magnetic minerals under different physicochemical conditions with the thermal magnetic analysis for BIFs and iron-ores collected from the Hamersley Province to fill the gap in knowledge highlighted by existing studies of the iron ores and BIFs. The results indicate that the high-grade hematite ores might have been undergone a physicochemical process under hydrothermal conditions between 120 °C and 220 °C during the major stage of enrichment from the original BIFs in the Brockman Iron Formation. Such physicochemical conditions would require either that the BIF units were buried 4000–5000 m underground with tilted broad channels formed by large-scale deformation in the region that facilitates hydrothermal reactions and leaching by the fluids flowing down deep to 4000–5000 m, somehow similar to the deep-seated supergene model proposed in previous works, or that the BIF units were still buried but the hydrothermal fluids coming up from deeper sources spread widely over the broad channels to ensure the high-grade hematite ores are consistently uniform over the entire deposit. The large-scale martite-goethite deposits in the Marra Mamba Iron Formation might be derived from multiple supergene phases from hematite-martite ores below 100 °C in the natural process of oxidization near surface, somewhat similar to the existing model for the channel iron deposits. Magnetite contained within current BIFs and iron ores was least likely derived from primary hematite in BIFs.

**Keywords:** Thermal magnetic analysis; high-grade hematite (martite) ores; martite-goethite ores; banded iron formation (BIF); physicochemical process; iron-ore genesis; Hamersley Province

---

## 1. Introduction

The Hamersley Province in the northwest section of Western Australia hosts one of the largest iron-ore reserves in the world. It is well-known for high-grade hematite ores derived from the extensive banded iron formations (BIFs) over the province. Studies in geology, mineralogy, geochemistry, petrophysics, and geophysics of the Hamersley Province have been documented since the 1960s [1–10]. Although arguments regarding the genesis of the iron ores have existed since this period [11–21], some facts seem widely accepted for the iron-ore deposits in the province, including the following:

- Regardless of their mineralization processes, the major ore types consist predominantly of martite (hematite) and martite-goethite ores;
- Regardless of the ore types, the iron ores likely derived from the original BIFs widely distributed in the Hamersley Province;
- The large-scale deformation or folding with the BIFs in the region likely played a key role in the enrichment of the iron ores from the BIFs, with various supergene, hypogene, and hydrothermal processes.

Mineralogical features of the iron ores and the hosting BIFs have been used as key evidence to support hypotheses of the origin of iron-ore deposits in the Hamersley Province directly by reflected light microscopy and indirectly by X-ray diffraction (XRD) [4,16,17,20–24] and thermal magnetism [6,7,25]. However, the sum of these results should be regarded as secondary evidence to infer the possible process of iron-ore enrichment in the province. This is because the ore and BIF samples under study largely represent the final status of the mineral composition, structure and texture of the samples, rather than the consecutive frames of the entire physicochemical processes of the ore enrichment. Therefore, the same result could have different interpretations depending on individuals' hypotheses under different assumptions. For example, by interpreting the reflected light photomicrographs of iron ores and BIFs from the Hamersley Province, Perring [20] proposed a four-stage process for the Hamersley martite-goethite mineralization that began from replacement of magnetite in original BIFs by hematite (or martitization) and ended with martite-goethite ores with relics of magnetite. For the reflected light photomicrographs of BIF drill-cores from the Hamersley Province, Tompkins and Cowan [22] interpreted that the primary hematite was reduced to magnetite during prograde regional metamorphism, which implied that the major magnetic minerals in the original BIFs in the Hamersley Province would be hematite, by citing the thermal magnetic data of the samples as supporting evidence. This view was in contrast to the thought that magnetite was likely the major magnetic mineral in the original BIFs [11,12,20,21].

In theory, mutual conversions between hematite and magnetite can happen more than once if the physicochemical conditions are favourable. Both XRD and thermal magnetic analyses only have the potential to indicate the current possible compositions of magnetic minerals contained in the samples, rather than directly linking to the previous processes that led to the current status of the samples. For instance, if a sample contains only hematite and magnetite, thermal magnetic analysis can only indicate the co-existence of magnetite and hematite in the sample, but it does not distinguish between the primary and secondary magnetite or hematite in the sample, unless new conversions occurred during the heating process up to 700 °C.

Even if mutual conversions between hematite and magnetite can happen in theory, the physicochemical conditions for the two-way conversions are vastly different in practice. The lack of consideration of the physicochemical conditions for the iron-ore enrichment from BIFs has been a weakness in many Hamersley iron-ore genesis models. Hence, this study aims to incorporate the latest research outcomes in conversions among the major magnetic minerals under different physicochemical conditions with the thermal magnetic analysis for BIFs and iron ores collected from the Hamersley Province to fill the gap in knowledge highlighted by existing studies of the iron ores and BIFs. The outcomes of this study would have an implication on further discussing the physicochemical viability of the existing iron-ore genesis models in the Hamersley Province.

Within this study, the classifications of Hamersley iron ores are summarized in Section 2, followed by the thermal magnetic experiments conducted on the Hamersley iron ores and BIFs in Section 3. Discussions are made in Section 4 based on the results from this study and existing sources in terms of better understanding of the possible processes of iron-ore enrichment in the Hamersley Province. A brief conclusion is made for this study in Section 5.

## 2. Classifications of the Hamersley iron ores

The Hamersley iron-ore deposits are mostly hosted in the BIFs of the Hamersley Group. The Hamersley Group contains eight formations as follows, in ascending order: Marra Mamba Iron Formation, Wittenoom Dolomite, Mount Sylvia Formation, Mount McRae Shale, Brockman Iron Formation, Weeli Wolli Formation, Woongarra Rhyolite, and Boolgeeda Iron Formation (Figure 1). BIFs are contained in the Marra Mamba Iron Formation, Mount Sylvia Formation, Brockman Iron Formation, Weeli Wolli Formation, and Boolgeeda Iron Formation; however, most high-grade iron ore deposits are hosted in the Brockman Iron Formation, approximately 620 m thick, and the Marra Mamba Iron Formation, approximately 230 m thick, with minor enrichments found in both the Weeli Wolli Formation and Boolgeeda Iron Formation. The Brockman Iron Formation consists of four members: Dales Gorge, Whaleback Shale, Joffre, and Yandicoogina Shale Members, in which large high-grade hematite ore deposits are commonly hosted in BIFs of both the Dales Gorge and Joffre members. The Marra Mamba Iron Formation has three members: Nammuldi, MacLeod, and Mount Newman Members, in which the iron-ore deposits are hosted mostly in the topmost Mount Newman Member, overlain by carbonate-rich rocks of the Wittenoom Dolomite. It has been reported that carbonate commonly exists in Marra Mamba BIFs and ores [20–22,26]. Additional detailed information regarding the regional geology in the Hamersley Basin can be found in classical works [4,5,11,12] and recent studies [16–21].

Prior to 2000, the Hamersley iron ores were described by many geologists [2–5,11,12], which led to the establishment of the Pilbara Iron Ore Classification (PIOC), mainly based on microscopic mineralogical and chemical studies. Iron ores that were rich in microplaty martite and free of goethite were classified as M-(mpl H) ores, which are mainly hosted in the Brockman BIFs (Figure 2). Martite is a term to denote hematite with the preserved crystal habit of the primary magnetite and was a diagnostic feature of the M-(mpl H) ore. Typical examples of these ores were found at the Tom Price and Mount Whaleback mines. Microplaty hematite ores in which significant goethite is present were classified as either martite-microplaty hematite-goethite ore or M-(mpl H)-g ore, and typically such ores were found at the Paraburdoo mine. Both the M-(mpl H) and M-(mpl H)-g ores are commonly hosted in the Brockman BIFs and hence can be called Brockman ores in general.

Goethite rich ores included Martite-Goethite (M-G) ores and Martite-ochreous Goethite type (M-oG) ores that contained a significant amount of ochreous goethite. Both the M-G and M-oG ores were commonly hosted in the Marra Mamba Iron Formation and are referred to as Marra Mamba ores. The average bulk density and magnetic susceptibility of the Hamersley iron ores were gradually decreasing from the M-(mpl H) ores, M-(mpl H)-g ores, M-G ores, and finally to M-oG ores [6,27].

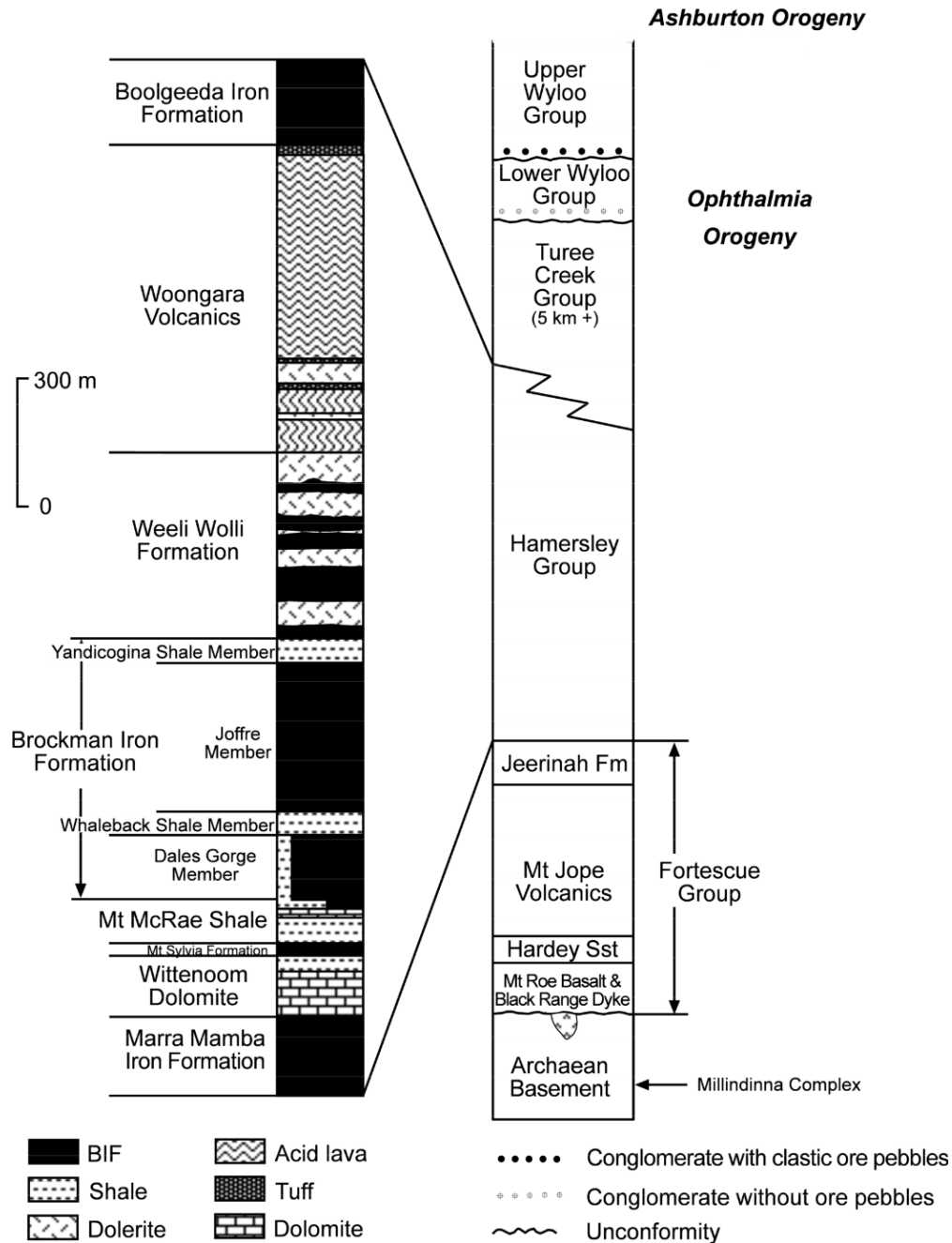


Figure 1. Stratigraphy in the Hamersley Province.

Microplaty hematite		Martite-goethite ores	
Tom Price and Whaleback mines	Paraburdoo mine	West Angelas A deposit	
M-(mpl H)	M-(mpl)-g	M-G	M-oG
Brockman ores		Mara Mamba ores	
← Increasing hematite		Increasing goethite →	

**Figure 2.** Pilbara Iron Ore Classification modified from [11,12].

Regardless of the microscopic features of the magnetic minerals contained in various types of iron ores, by means of the chemical compositions of hematite (martite) and goethite in the iron ores, a simplified classification of the Hamersley iron ores was proposed by Clout in 2006 [16], which is summarized in Figure 3. Thermal magnetic analysis would be more aligned to this new classification as the thermal treatment of rock and ore samples is actually a physicochemical process, regardless of the colour, pseudomorphs, and porosity of the minerals contained in the samples.

Hardness	Main magnetic minerals in iron ores				Porosity
	Hematite	Hematite-Goethite	Goethite-Hematite	Goethite	
Hard	X	X			Increasing ↓
Medium	X	X	X	X	
Friable	X	X	X	X	
Powder/dust	X		X	X	
	← Increasing hematite content				

**Figure 3.** Textural classifications of Hamersley iron ores modified from [16].

Although magnetite exists in most of the iron ores regardless of its primary or secondary nature, the ore classifications do not include magnetite due to its tiny proportion in weight percentage in the ores. However, because magnetite (or maghemite) is hundreds of times stronger in magnetism than any other magnetic minerals in the ores, the presence of magnetite with even 0.1 wt% in the ores would be clearly shown in the thermal magnetic experiments [6,7,25].

### 3. Results of the thermal magnetic experiments with the Hamersley iron ores and BIFs

#### 3.1. Background and related information about the thermal magnetic analysis

A magnetic mineral will lose magnetism if it is heated to a temperature that is commonly called the Curie temperature of that mineral. This is because the original magnetic orientation carried by the mineral will be destroyed at its Curie temperature [28–31]. In practice, most magnetic minerals would be demagnetized gradually within a temperature range roughly around the Curie temperature due to the differences in grain size of a mineral, purity of the mineral, mixture of multiple minerals, or the combination of all these factors. Hence, despite the availability of the Curie temperatures for the common magnetic minerals in various sources, they should be regarded as references only

because of the diversity in chemical composition and physical conditions of individual samples under the experiment. Summarized from many known sources [28–39], Table 1 serves as a reference to the Curie temperature (range) and mass susceptibility of each of the likely magnetic minerals or the minerals contained in the iron ores and BIFs that could be converted to magnetic minerals during heating. It should be noted that this table is not exclusive of the results from other sources, particularly the mass susceptibility that has a wide range in the reported data from different sources. As a result, this study utilizes the normalized magnetic susceptibility by the maximum value observed during heating (or cooling) during the thermal magnetic analysis instead of the actual mass susceptibility.

**Table 1.** Some generalized properties of ferromagnetic minerals.

Minerals	Composition	Curie temperature (°C)	Mass susceptibility ( $\times 10^{-6}$ SI/kg)
Magnetite	Fe <sub>3</sub> O <sub>4</sub>	575–580	200–1100
Maghemite	$\gamma$ -Fe <sub>3</sub> O <sub>4</sub>	Unstable	400–500
Hematite	$\alpha$ -Fe <sub>2</sub> O <sub>3</sub>	675	0.1–7.6
Goethite	$\gamma$ -FeOOH	120–130	0.3–2.8
Pyrrhotite	Fe <sub>7</sub> S <sub>8</sub>	320	0.1–300
Pyrite	FeS <sub>2</sub>	Unstable	0.01–1
Siderite	FeCO <sub>3</sub>	400–530	0.32–2.7

If a sample contains unstable magnetic minerals (e.g., maghemite), iron sulphides (e.g., pyrrhotite and pyrite), or iron carbonates (e.g., siderite), gradually heating the sample in air will induce chemical reactions with these minerals, resulting in some stable secondary magnetic minerals, commonly either magnetite or hematite. The conversion temperature or temperature range varies with the minerals. Some chemical reactions involving these magnetic minerals are summarized in Table 2, compiled from various references.

**Table 2.** Thermochemical reactions involving magnetic minerals.

Initial mineral	Alteration product	Converting temperature (°C)
Maghemite	Hematite	350–450
Pyrrhotite	Magnetite	>500
Pyrite	Magnetite	350–500
Lepidocrocite	Maghemite	220–270
Goethite	Hematite (without carbon)	350–600
	Magnetite (with carbon)	350–580
Siderite	Magnetite	>200

All the thermal magnetic experiments reported in this study were carried out in an open room environment with powders of selected iron-ore and BIF samples using a Bartington MS2 susceptibility system. The powders were not sealed in a vacuum container during both heating and cooling stages so as to observe the difference between demagnetization and remagnetization of unstable magnetic minerals and possible iron sulphides or carbonates contained in the samples

during the experiment. The maximum heating temperature was set to 710 °C. Thermal susceptibility measurements were operated within a magnetic shield.

For the purpose of mutual validation, the spare powders of some samples selected for the thermal magnetic analysis were also sent for XRD analysis. The XRD results are summarized in Table 3 as a general reference.

**Table 3.** Summary of XRD results of the Hamersley iron ores and BIFs [6].

	Hematite ore	Hematite-Goethite ore	Fresh BIF	Weathered BIF
Magnetite (wt%)	–	–	>10	<1–12
Hematite (wt%)	>99	62–74	>20	20–70
Goethite (wt%)	–	5–32	<5	2–31
Sulphur (ppm)	–	<10–180	–	<10–1020

### 3.2. Results of the thermal magnetic experiments on the iron ores

#### 3.2.1. Hematite ores

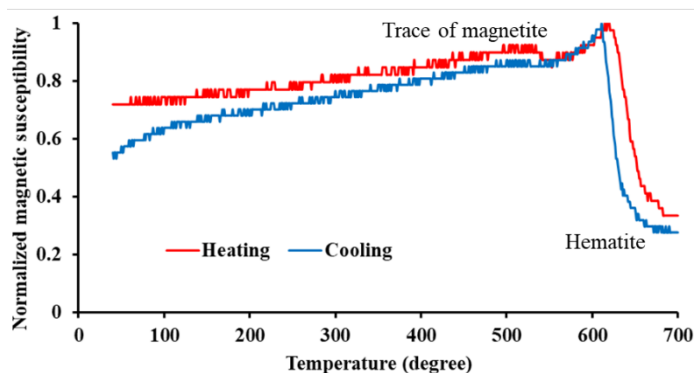
The XRD results in Table 3 indicate that the high-grade hematite ores contain more than 99% of hematite (or martite) with magnetite, goethite, and sulphur, all below the detecting threshold. The thermal magnetic experiments confirm that little to no goethite and iron sulphides existed in all high-grade hematite ores from the Mount Whaleback, Top Price, and Paraburdoo mines (Figure 4).

However, a trace of magnetite exists in the high-grade hematite ores, as indicated by a drop in the heating curve and a jump in the cooling curve of the magnetic susceptibility around 570 °C. As the magnetic susceptibility is normalized, the relative magnitude of the drop (and jump) may indicate that the amount of magnetite increases slightly from the Mount Whaleback ore to the Tom Price ore and to the Paraburdoo ore, even though the amount is still too small to be detected by XRD. The trace of magnetite in the high-grade hematite ores would likely be the relict primary magnetite contained in the original BIFs because no chemical reaction occurred during both the heating and cooling processes. This is consistent with the microscopic observations reported by Morris [11].

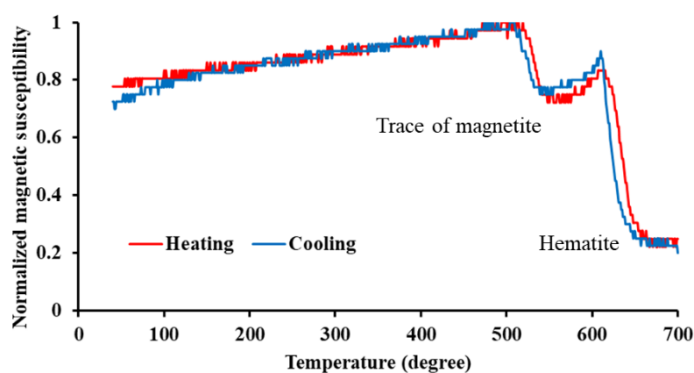
#### 3.2.2. Hematite-goethite ores

The XRD results in Table 3 indicate that the hematite-goethite ores may contain more than 60% of hematite, 5–32% of goethite, and possibly a trace of iron sulphides or carbonates, though the amount of magnetite is likely below the detecting threshold. During heating (Figure 5), chemical conversion occurred from 350 °C to 560 °C (the red line) that caused a dramatic increase in magnetic susceptibility. The heating curve showed a sharp drop in magnetic susceptibility around 570 °C, which indicates that either goethite or some portion of the goethite should have been converted to magnetite. The jump in magnetic susceptibility in the cooling curve around 650 °C, compared to the invisible dip in magnetic susceptibility in the heating curve, indicates a slight increase in hematite after heating, which would likely result from the combination of the primary hematite originally in the hematite-goethite ore and the secondary hematite partly converted from the goethite during heating. This thermal magnetic pattern is very similar to one recently reported by Till and Nowaczyk [34], who demonstrated that

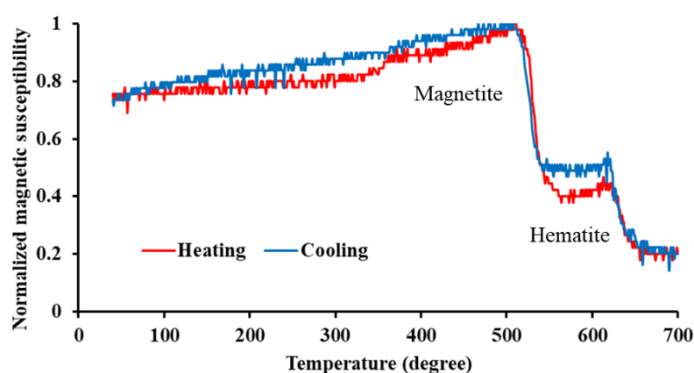
goethite could be converted either to magnetite when carbon existed or to hematite when carbon was scarce during heating from 350 °C to 600 °C. With the formation of the secondary magnetite (hematite too) after heating, the cooling process ended with a much high magnetic susceptibility compared with the initial status.



(a) Mount Whaleback hematite ore.



(b) Tom Price hematite ore.



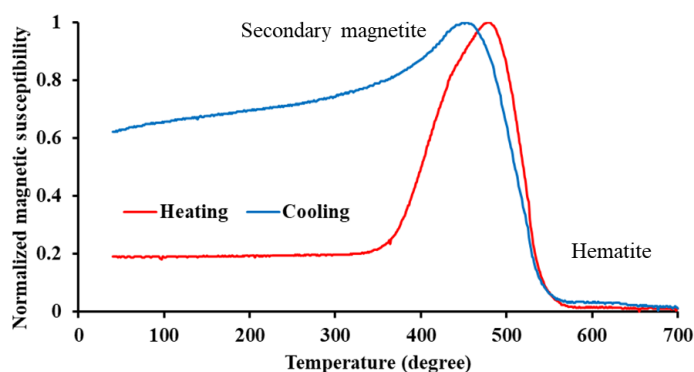
(c) Paraburdoo hematite ore.

**Figure 4.** Thermal susceptibility curve of hematite ore.

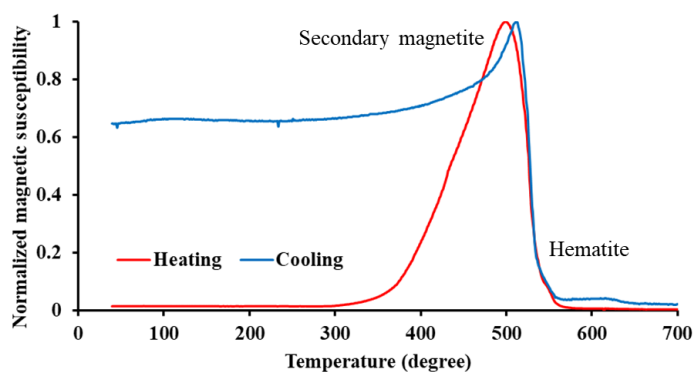
However, where the carbon comes from during the chemical reactions becomes a key question to support the conversion of goethite to magnetite. Pan et al. [33] reported a similar thermal magnetic pattern of conversion from siderite, an iron carbonate, to magnetite during heating from 350 °C to 600 °C in air (i.e.,  $3\text{FeCO}_3 + \text{H}_2\text{O} \rightarrow \text{Fe}_3\text{O}_4 + 3\text{CO}_2 + \text{H}_2$ ). As the amount of siderite in the hematite-goethite ores is smaller than the threshold of XRD detection, the limited amount of  $\text{CO}_2$



released from the siderite conversion can help convert some of the goethite to magnetite whereas the rest of the goethite would be converted to hematite. This should be a more reasonable interpretation than the earlier interpretations in [25].



(a) West Angelas hematite-goethite ore.

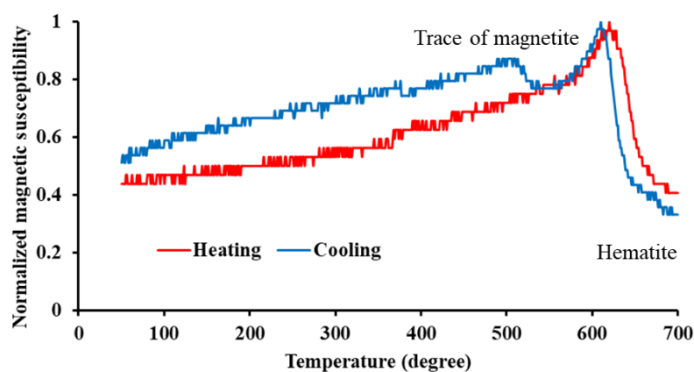


(b) Area C hematite-goethite ore.

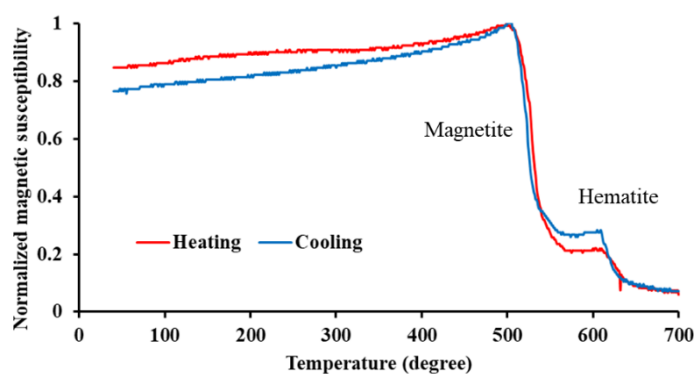
**Figure 5.** Thermal susceptibility curve of hematite-goethite ore.

### 3.2.3. Other iron ores from the Hamersley Province

There are many small-medium iron-ore deposits in the Hamersley Province. Local enrichment as hematite pebble conglomerates were found in the Mount McGrath Formation of the middle Whyloo Group. The hematite pebbles were originated from the Brockman high-grade hematite ores that were physically moved downstream by seasonal floods and then deposited in the catchment area in the younger Mount McGrath Formation. Later, physical and chemical processes, likely in a low-temperature environment, formed the hematite pebble conglomerates. The XRD result from the hematite pebble samples showed that the hematite pebbles contain more than 96% of hematite with a trace of sulphur around 100 ppm, though magnetite and goethite are below the detecting threshold. The thermal magnetic analysis showed that no observable primary magnetite was contained in the hematite pebble in the heating curve (Figure 6a) beside the dominance of hematite. However, in the cooling curve, a trace of magnetite occurred around 560 °C (the blue line). This indicated that a trace of secondary magnetite was formed from a trace of iron sulphides during heating. Such chemical conversion was too subtle to be observed due to the tiny amount of sulphur released during heating.



(a) Hematite conglomerate from Mount McGrath Formation of Whyloo Group.



(b) Recrystallized magnetite-hematite ore from Channer mine.

**Figure 6.** Thermal susceptibility curve of other iron ores.

A recrystallized magnetite-hematite ore from the Channer mine was also studied by thermal magnetic analysis. The sample was collected from the contact zone of a later dyke crossing through the hematite (martite) ores. A significant proportion of the hematite was recrystallized to magnetite that could be seen by naked eye and was able to pull small iron objects towards the recrystallized ore sample. The heating and cooling curves showed a consistent pattern of dominance by both the recrystallized magnetite and the primary hematite (Figure 6b). This indicates that the inverse conversion from hematite to magnetite is possible under the extreme high-temperature hydrothermal conditions, even though not all hematite could be converted to magnetite.

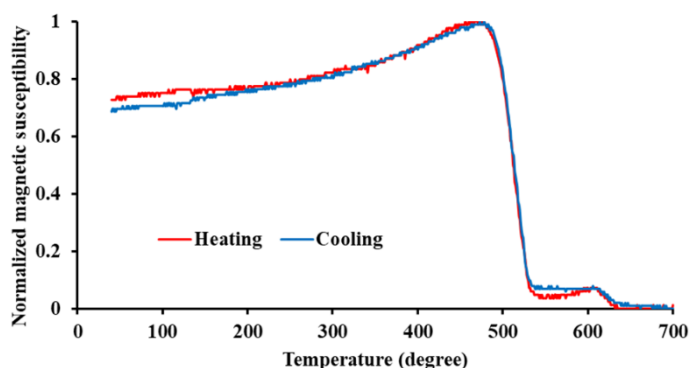
### 3.3. Results of the thermal magnetic experiments on the BIFs

#### 3.3.1. Fresh and lowly weathered BIFs

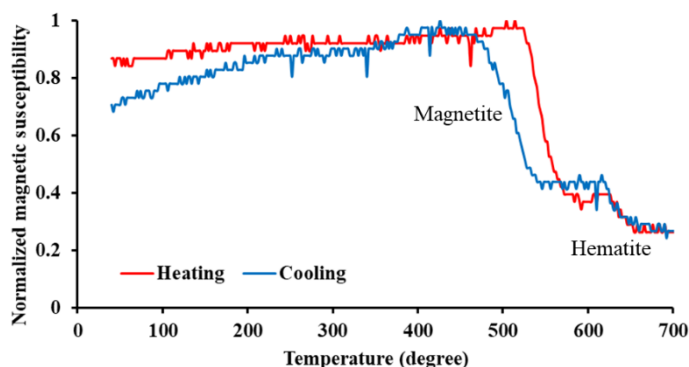
Fresh BIF outcrops were only found in the current open pits and in a few deep cliffs of recent road cuts, even though most solid samples collected from such sites were still subject to low-medium weathering effect with 30–50% hematite and 2–12% magnetite.

The few fresh BIF samples exhibited a magnetic pattern similar to the recrystallized magnetite ore shown in Figure 6b (i.e., a clear indication of both magnetite and hematite) (Figure 7). Despite the similarity in the thermal magnetic pattern between the fresh BIFs and the recrystallized magnetite ore, the magnetite contained in the fresh BIFs are likely the primary magnetite, of which a large

proportion would have been altered to hematite. This is opposite to the process of conversion from hematite to magnetite of the recrystallized magnetite ore, even though both shared a similar thermal magnetic pattern.



(a) Fresh BIF of the Brockman Iron Formation from an open pit.



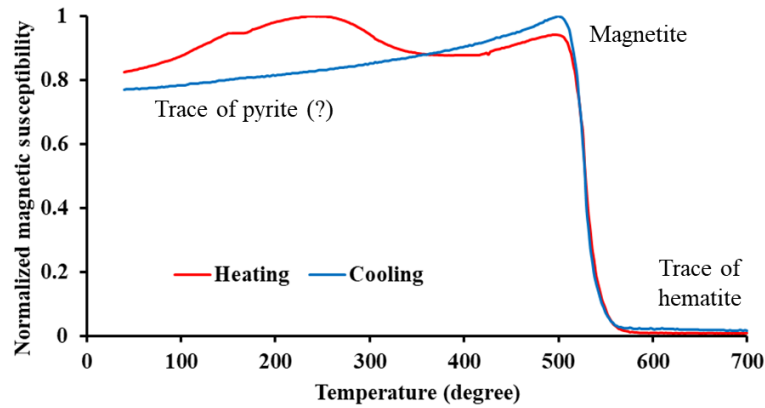
(b) Fresh BIF of the Brockman Iron Formation from a recent road cut.

**Figure 7.** Thermal susceptibility curve of fresh BIFs.

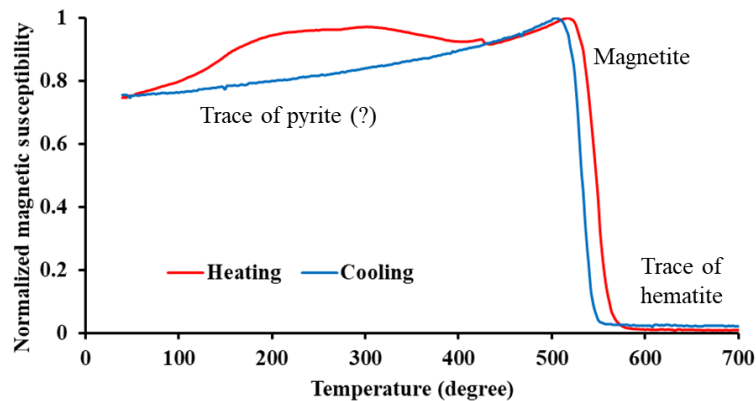
Lowly weathered BIF samples collected from roadsides showed that a trace of iron sulphides coexisted with magnetite and hematite in the thermal magnetic curves (Figure 8). The small change in magnetic susceptibility from 100 °C up to 400 °C may indicate a small degree of chemical reactions from pyrite to magnetite. Such a pattern is consistent with the thermal magnetic experiment on pyrite reported by Wang et al. [32]. The possible chemical reaction was enabled by the existence of 70–100 ppm of sulphur detected by the XRD analysis.

### 3.3.2. Highly weathered BIFs

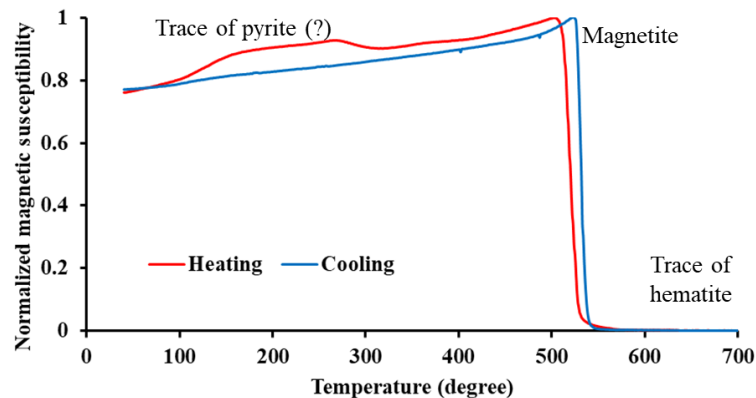
It seemed that the highly weathered surface BIF samples had roughly two thermal magnetic patterns. The first pattern indicated the coexistence of primary magnetite, its partially oxidized alteration of maghemite, and fully oxidized product of hematite (Figure 9). This pattern seemed common in all BIF units, except for the Mara Mamba Iron Formation. The existence of maghemite was indicated by the small increase in magnetic susceptibility from 100 °C up to 275 °C, as seen in the heating curve, and then a small drop in magnetic susceptibility above 275 °C, where maghemite would have been converted to less magnetic hematite. This behaviour is consistent with the recent physicochemical experiments reported by Li et al. [40].



(a) Lowly weathered BIF of the Willi Wollli Formation from Tom Price area.



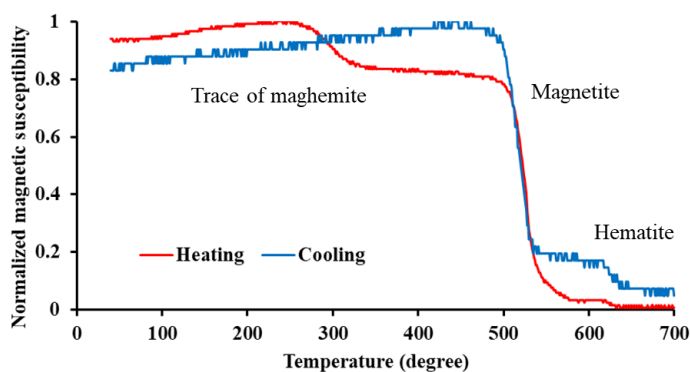
(b) Lowly weathered BIF of the Brockman Iron Formation from Newman area.



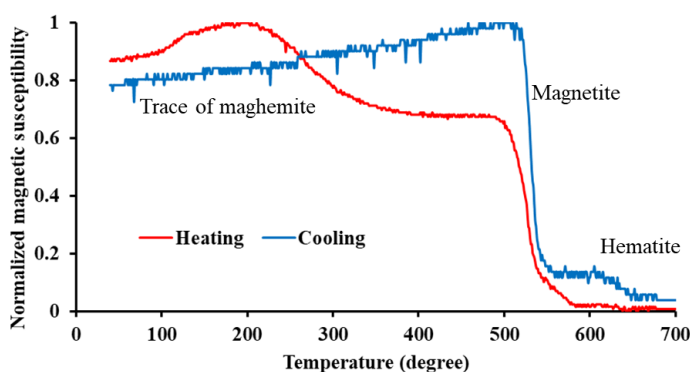
(c) Lowly weathered BIF of the Mount Sylvia Formation from the Hamersley Range.

**Figure 8.** Thermal susceptibility curve of lowly weathered BIFs.

The second thermal magnetic pattern seemed common for the highly weathered BIF samples from the Mara Mamba Iron Formation (Figure 10a-b), although the locally mineralized BIF sample with about 60 wt% of hematite and 10 wt% of goethite in the Boolgeeda Iron Formation also shared the same pattern (Figure 10c). This is similar to the pattern exhibited by the hematite-goethite ores hosted in the Mara Mamba BIFs (Figure 5). This indicates that supergene iron carbonates and iron sulphides are likely present in the highly weathered BIFs, thus pointing to the similar origin to the hematite-goethite ores.



(a) Weathered BIF of Boolgeeda Iron Formation from Tom Price area.



(b) Weathered BIF of the Brockman Iron Formation from the Newman area.

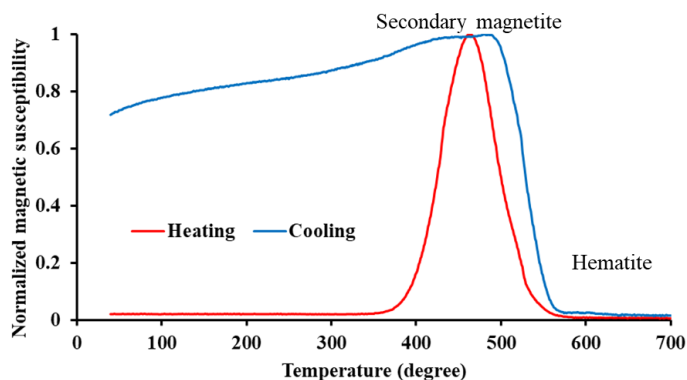
**Figure 9.** First thermal magnetic pattern of highly weathered BIFs.

## 4. Discussion

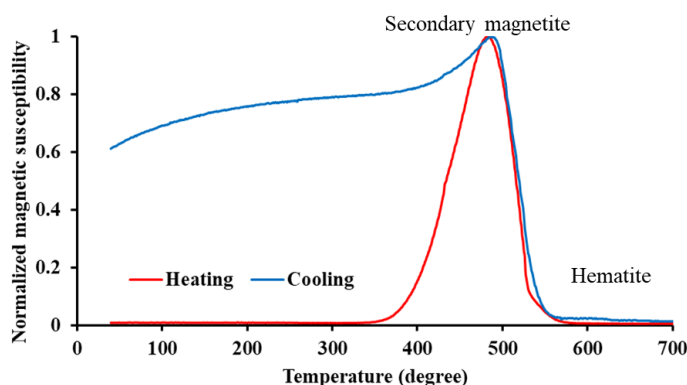
### 4.1. Possible physicochemical processes of the hematite ores in the Hamersley Province

Physicochemical experiments reported in [40] showed that, under hydrothermal conditions, magnetite was oxidized to a high concentration of maghemite and hematite between 120 °C and 180 °C, whereas magnetite was converted to hematite directly with no specific morphologies at 275 °C. Zhao et al. [41] also found that, under hydrothermal conditions, magnetite was replaced by hematite between 140 °C and 220 °C, with a fast reaction rate at around 200 °C. This study also reported that oxygen was not an essential factor for the reaction, although sufficient oxidant would trigger the reaction. Both studies did not observe the formation of goethite during the experiments.

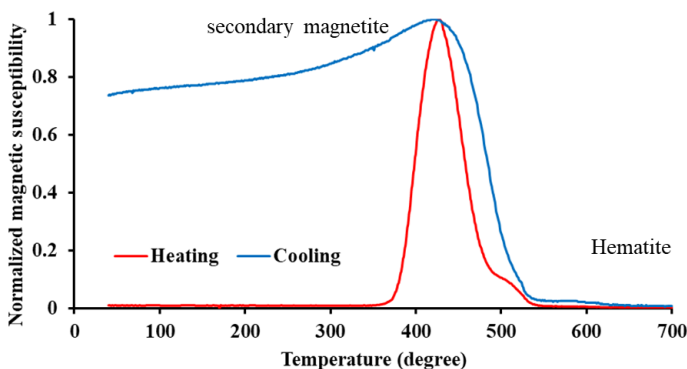
The high-grade hematite ores from the Mount Whaleback and Tom Price mines are martitized with the original crystal habit of magnetite and contains no goethite. These features are similar to the hematite converted from magnetite through the physicochemical process under hydrothermal conditions between 120 °C and 220 °C reported in the above studies. This similarity may imply that the high-grade hematite ores in the Hamersley Province might have undergone a similar physicochemical process under similar hydrothermal conditions during the major stage of enrichment from the original BIFs in the Brockman Iron Formation. If this hypothesis is reasonable, the similar conditions would be possible in one of the following two circumstances or their combination during the major enrichment stage.



(a) Weathered BIF of the Mara Mamba Iron Formation from Newman area.



(b) Weathered BIF of the Mara Mamba Iron Formation from Tom Price area.



(c) Locally mineralized BIF of the Boolgeeda Iron Formation from the Tom Price area.

**Figure 10.** Second thermal magnetic pattern of highly weathered BIFs.

First, the BIF units were buried 4000–5000 m underground with tilted broad channels formed by large-scale deformation in the region that would facilitate the hydrothermal reactions and leaching the cherty materials away. By a common thermal gradient of 15–30 °C/km for the crust, fluids flowing down to 4000–5000 m deep would be around 60 °C to 150 °C with the required hydrothermal conditions to some extent. This assumption is somehow similar to the deep-seated supergene model of high-grade martite-hematite ores proposed in [4,11,12]. A logical inference can be made in which the small proportion of goethite in the Parabudoo hematite ores might be the later alteration of hematite to goethite during uplifts of the buried hematite deposits.

Second, the BIF units were still buried, but the hydrothermal fluids would come up from deeper sources to enable the similar physicochemical process. Additionally, the hydrothermal fluids must be wide spread over the broad channels to ensure the high-grade hematite ores with a uniform consistency over the entire deposit, rather than a thin channel from which the hydrothermal fluids would create physical gradients whilst spreading. If the process did not occur widely underground, a complex of minerals would be present in the ores from different zones, rather than solely the high-grade hematite.

#### *4.2. Possible physicochemical processes of the hematite-goethite ores in the Hamersley Province*

Magnetite in BIFs would be gradually altered to maghemite and then to hematite below 100 °C in the natural process of oxidization near the surface. Further alterations with other chemicals in rocks and fluids near the surface would convert some hematite to goethite, iron sulphides, and iron carbonates. This is evidenced in the thermal magnetic curves shown in Figure 5. These multiple phased mutual alternations would either lead BIFs to martite-goethite ores directly or high-grade hematite ores to martite-goethite ores under suitable conditions.

The large-scale martite-goethite deposits in the Marra Mamba Iron Formation might be derived from multiple later supergene phases from the hematite-martite ores formed earlier through a similar hydrothermal process as suggested above. This seems somewhat similar to the genesis model for the channel iron deposits proposed in [20,21]. The small local martite-goethite deposits occurred in the surface BIFs of the Boolgeeda Iron Formation (Weeli Wolli Formation too) share a similar thermal magnetic pattern to the Marra Mamba martite-goethite ores (Figure 10c); however, they would likely be formed from either multiple phased mutual alternations or weathering near surface directly, which is the same magnetic pattern shared by unmineralized and highly weathered BIFs in the Marra Mamba Iron Formation (Figure 10a-b).

#### *4.3. Magnetite sources in BIFs and ores in the Hamersley Province*

According to [42,43], hematite can be converted to magnetite with carbon oxides between 400 °C and 600 °C. However, the crystal structure of the hematite was completely destroyed during the chemical reactions and the magnetite formed was not in its usual crystal structure. This seems contradictory to the suggestion that the magnetite in the Hamersley BIFs was derived from the primary hematite in [22]. This is because the typical crystal structure of magnetite was still observable under microscopy in both the Hamersley BIFs and hematite ores [11,12]. Undeniably, magnetite contained in the current BIFs and iron ores should come from multiple sources; for example, the primary magnetite in the fresh BIFs, the tiny amount magnetite relicts in the iron ores, and altered secondary magnetite from siderite, maghemite, goethite, pyrite, evidenced in the thermal magnetic curves of BIF and ore samples shown in Figures 5–10. The least likely pathway was that the magnetite in the BIFs were derived from the primary hematite in the “original” BIFs.

## **5. Conclusions**

The genesis of the iron ores hosted in BIFs in the Hamersley Province of Western Australia has been argued since the iron-ore deposits were discovered in the 1960s; for example, various supergene, hypogene, and hydrothermal processes being among the popular models. These models were largely

based on geological inferences incorporating evidence from chemical analysis, X-ray diffraction (XRD) analysis, microscopic observations, rock magnetic and/or paleomagnetic interpretations for various types of iron-ores, and hosting BIFs. Mineralogical features of the current iron ores and the hosting BIFs are indeed important in supporting any hypothesis of the origin of iron-ores, but their interpretation should consider the likely physicochemical conditions that were necessary during the iron enrichment from the BIFs to the high-grade iron ores. The lack of consideration of the physicochemical conditions in iron-ore enrichment from BIFs has been a weakness of many Hamersley iron-ore genesis models. Hence, this study aimed to incorporate the latest research outcomes in conversions among the major magnetic minerals under different physicochemical conditions with the thermal magnetic analysis for BIFs and iron ores collected from the Hamersley Province to fill the gap in knowledge highlighted by existing studies of Hamersley iron ores and BIFs.

Regarding the high-grade hematite ores in the Hamersley Province, this study indicates that these ores might have undergone a physicochemical process with hydrothermal conditions between 120 °C and 220 °C during the major stage of enrichment from the original BIFs in the Brockman Iron Formation. Such physicochemical conditions would be formed in one of the two circumstances (or their combination) during the major enrichment stage. The BIF units were buried 4000–5000 m underground with tilted broad channels formed by large-scale deformation in the region that would facilitate the hydrothermal reactions and leach the cherty materials away by flowing fluids down deep to 4000–5000 m, which is somehow similar to the deep-seated supergene genesis model of high-grade martite-hematite ores proposed in [4,11,12]. Alternatively, the BIF units were still buried, but the hydrothermal fluids would come up from deeper sources to enable the similar physicochemical process. However, this requires that the hydrothermal fluids spread widely over the broad channels to ensure the high-grade hematite ores with a consistent uniformity over the entire deposit as shown in the Mount Whaleback and Tom Price mines. If the wide-spreading process did not occur underground, a complex of minerals would be present in the ores, rather than solely in the high-grade hematite.

Magnetite in BIFs would be gradually altered to maghemite and then hematite below 100 °C in the natural process of oxidization near surface. Further alterations with other chemicals in rocks and fluids near the surface would convert some hematite to goethite, iron sulphides and iron carbonates. Hence, the large-scale martite-goethite deposits in the Marra Mamba Iron Formation might be derived from multiple later supergene phases from the hematite-martite ores formed earlier. This seems somewhat similar to the genesis model for the channel iron deposits proposed in [20,21].

When hematite is converted to magnetite with carbon oxides between 400 °C and 600 °C, the crystal structure of the hematite was completely destroyed during the chemical reactions and the magnetite formed was not in its usual crystal structure. Hence, the magnetite in the BIFs was derived from the primary hematite in the “original” BIFs would be the least likely pathway for the Hamersley BIFs.

The limitation of this study is the lack of a systematic association with the inferred physicochemical conditions, under which the possible geological evolution of the Hamersley BIFs and iron ores could be observed. This requires a future collaborative project involving experts from all related areas to work together.

## Acknowledgments

Much of the original work was supported by the Minerals & Energy Research Institute of WA, BHP, Rio Tinto, and The University of Western Australia. Special thanks go to Professor Z-X Li



for his guidance and help during the field trips, sample collections, and rock magnetic experiments for a paleomagnetic project.

### Conflict of interest

The author declare no conflict of interest.

### References

1. Blockley JG (1969) *The stratigraphy of the Mount Tom Price orebody and its implication in the genesis of iron ore*. Western Australia Geological Survey Annual Report 1968. Perth, Australia: Western Australia Geological Survey.
2. Ayers DE (1971) The hematite enrichment ores of Mount Tom Price and Mount Whaleback. *Aust Inst Min Metall Proc* 238: 47–58.
3. Trendall AF, Pepper RS (1977) *Chemical composition of the Brockman Iron Formation*. Perth, Australia: Western Australia Geological Survey.
4. Morris RC (1980) A textural and mineralogical study of the relationship of iron ore to banded iron-formation in the Hamersley iron province of Western Australia. *Econ Geol* 75: 184–209. <https://doi.org/10.2113/gsecongeo.75.2.184>
5. Kneeshaw M (1984) Pilbara iron ore classification—a proposal for a common classification for BIF-derived supergene iron ore. *Australas Inst Min Metall* 289: 157–162.
6. Guo WW (1999) *Magnetic petrophysics and density investigations of the Hamersley Province, Western Australia: implications for magnetic and gravity interpretation*, Australia: The University of Western Australia.
7. Li ZX, Guo W, Powell CMA (2000) *Timing and genesis of Hamersley BIF-hosted iron deposits: a new palaeomagnetic interpretation*, Perth, Australia: Minerals & Energy Research Institute of Western Australia.
8. Thorne WS, Hagemann SG, Barley M (2004). Petrographic and geochemical evidence for hydrothermal evolution of the North Deposit, Mt Tom Price, Western Australia. *Miner Deposita* 39: 766–783. <https://doi.org/10.1007/s00126-004-0444-x>
9. Bodycoat FM (2010) Stratigraphic and structural setting of iron mineralization at E Deposit (East), Area C, Hamersley Province, Western Australia. *Appl Earth Sci* 119: 49–55. <https://doi.org/10.1179/037174510X12853354810543>
10. Clark DA, Foss CA, Austin J, et al. (2015) Three-dimensional mapping of magnetite and hematite concentrations from reprocessing of detailed aeromagnetic data. *Proceedings of the Iron Ore Conference*, Perth, Australia.
11. Morris RC (1985) Genesis of iron ore in banded iron-formation by supergene and supergene–metamorphic processes—a conceptual model, In: Wolf KH, Eds., *Handbook of strata-bound and stratiform ore deposits*, Elsevier, 73–235.
12. Harmsworth RA, Kneeshaw M, Morris RC, et al. (1990) BIF-derived iron ores of the Hamersley Province. *Australas Inst Min Metall Mono* 14: 617–642.
13. Barley M, Pickard AL, Hagemann S, et al. (1999). Hydrothermal origin for the 2 billion year old Mount Tom Price giant iron ore deposit, Hamersley Province, Western Australia. *Miner Deposita* 34: 784–789. <https://doi.org/10.1007/s001260050238>

14. Powell CMcA, Oliver NHS, Li ZX, et al. (1999) Synorogenic hydrothermal origin for giant Hamersley iron oxide ore bodies. *Geology* 27: 175–178. [https://doi.org/10.1130/0091-7613\(1999\)027<0175:SHOFGH>2.3.CO;2](https://doi.org/10.1130/0091-7613(1999)027<0175:SHOFGH>2.3.CO;2)
15. Brocks JJ, Summons RE, Buick R, et al. (2003) Origin and significance of aromatic hydrocarbons in giant iron ore deposits of the late Archean Hamersley Basin, Western Australia. *Org Geochem* 34: 1161–1175. [https://doi.org/10.1016/S0146-6380\(03\)00065-2](https://doi.org/10.1016/S0146-6380(03)00065-2)
16. Clout JMF (2006) Iron formation-hosted iron ores in the Hamersley Province of Western Australia. *Appl Earth Sci* 115: 115–125. <https://doi.org/10.1179/174327506X138931>
17. Morris RC, Kneeshaw M (2011) Genesis modelling for the Hamersley BIF-hosted iron ores of Western Australia: a critical review. *Aust J Earth Sci* 58: 417–451. <https://doi.org/10.1080/08120099.2011.566937>
18. White AJR, Legras M, Smith RE, et al. (2014) Deformation-driven, regional-scale metasomatism in the Hamersley Basin, Western Australia. *J Metamorphic Geol* 32: 417–433. <https://doi.org/10.1111/jmg.12078>
19. Perring C, Crowe M, Hronsky J (2020). A new fluid-flow model for the genesis of banded iron formation-hosted martite–goethite mineralization, with special reference to the North and South Flank deposits of the Hamersley Province, Western Australia. *Econ Geol* 115: 627–659. <https://doi.org/10.5382/econgeo.4734>
20. Perring CS (2021) Petrography of martite–goethite ore and implications for ore genesis, South Flank, Hamersley Province, Western Australia. *Aust J Earth Sci* 68: 782–798. <https://doi.org/10.1080/08120099.2021.1863860>
21. Perring CS, Hronsky JMA, Crowe M (2022) Phanerozoic history of the Pilbara region: implications for iron mineralization. *Aust J Earth Sci* 69: 757–775. <https://doi.org/10.1080/08120099.2022.2048888>
22. Tompkins LA, Cowan DR (2001) Opaque mineralogy and magnetic properties of selected banded iron-formations, Hamersley Basin, Western Australia. *Aust J Earth Sci* 48: 427–437. <https://doi.org/10.1046/j.1440-0952.2001.00869.x>
23. Rasmussen B, Muhling JR (2018) Making magnetite late again: Evidence for widespread magnetite growth by thermal decomposition of siderite in Hamersley banded iron formations. *Precambrian Res* 306: 64–93. <https://doi.org/10.1016/j.precamres.2017.12.017>
24. Warchola T, Lalonde SV, Pecoits E, et al. (2018) Petrology and geochemistry of the Boolgeeda Iron Formation, Hamersley Basin, Western Australia. *Precambrian Res* 316: 155–173. <https://doi.org/10.1016/j.precamres.2018.07.015>
25. Guo WW (2015) Magnetic mineralogical characteristics of Hamersley iron ores in Western Australia. *J App Math Phys* 3: 150–155. <http://dx.doi.org/10.4236/jamp.2015.32023>
26. Blockley JG, Tehnas IJ, Mandyczewsky A, et al. (1993) *Proposed stratigraphic subdivision of the Marra Mamba Iron formation and the lower Wittenoom Dolomite*, Geological Survey of Western Australia Report 34. Perth, Australia: Western Australia Geological Survey.
27. Guo W (2023) Density investigation and implications for exploring iron-ore deposits using gravity method in the Hamersley Province, Western Australia. *AIMS Geosci* 9: 34–48. <https://doi.org/10.3934/geosci.2023003>
28. Tarling DH, Hrouda F (1993) *The Magnetic Anisotropy of Rocks*, London, UK: Chapman & Hall.
29. Dunlop DJ, Ozdemir O (1997) *Rock Magnetism*, Cambridge University Press, Cambridge, UK: <http://dx.doi.org/10.1017/CBO9780511612794>
30. Thompson R, Oldfield E (1986) *Environmental Magnetism*, London, UK: Allen and Unwin. <http://dx.doi.org/10.1007/978-94-011-8036-8>

31. Hunt, CP, Moskowitz BM, Banerjee SK (1995) Magnetic properties of rocks and minerals, In Ahrens TJ, Eds., *Rock Physics and Phase Relations: A Handbook of Physical Constants*, Vol. 3. Washington, DC: American Geophysical Union, 189–204.
32. Wang L, Pan Y, Li J, et al. (2008) Magnetic properties related to thermal treatment of pyrite. *Sci China Ser D-Earth Sci* 51: 1144–1153. <https://doi.org/10.1007/s11430-008-0083-7>
33. Pan Y, Zhu R, Liu Q, et al. (1999) Magnetic susceptibility variation and AMS exchange related to thermal treatment of siderite. *Chin Sci Bull* 44: 1135–1139. <https://doi.org/10.1007/BF02886143>
34. Till JL, Nowaczyk N (2018) Authigenic magnetite formation from goethite and hematite and chemical remanent magnetization acquisition. *Geophys J Int* 213: 1818–1831. <https://doi.org/10.1093/gji/ggy083>
35. Ouyang T, Appel E, Jia G et al. (2013) Magnetic mineralogy and its implication of contemporary coastal sediments from South China. *Environ Earth Sci* 68: 1609–1617. <https://doi.org/10.1007/s12665-012-1854-1>
36. Ter Maat GW, McEnroe SA, Church NS, et al. (2019). Magnetic mineralogy and petrophysical properties of ultramafic rocks: Consequences for crustal magnetism. *Geochem Geophys Geosyst* 20: 1794–1817. <https://doi.org/10.1029/2018GC008132>
37. Zhao XY, Liu QS (2010) Effects of the grain size distribution on the temperature-dependent magnetic susceptibility of magnetite nanoparticles. *Sci China Earth Sci* 53: 1071–1078. <https://doi.org/10.1007/s11430-010-4015-y>
38. Carlut J, Isambert A, Bouquerel H, et al. (2015) Low temperature magnetic properties of the Late Archean Boolgeeda iron formation (Hamersley Group, Western Australia): environmental implications. *Front Earth Sci* 3. <https://doi.org/10.3389/feart.2015.00018>
39. Henry B, Jordanova D, Jordanova N, et al. (2005) Transformations of magnetic mineralogy in rocks revealed by difference of hysteresis loops measured after stepwise heating: theory and case studies, *Geophys J Int* 162: 64–78. <https://doi.org/10.1111/j.1365-246X.2005.02644.x>
40. Li Z, Chanéac C, Berger G, et al. (2019) Mechanism and kinetics of magnetite oxidation under hydrothermal conditions. *RSC Adv* 58: 33633–33642. <https://doi.org/10.1039/c9ra03234g>
41. Zhao J, Brugger J, Pring A (2019) Mechanism and kinetics of hydrothermal replacement of magnetite by hematite. *Geosci Front* 10: 29–41. <https://doi.org/10.1016/j.gsf.2018.05.015>
42. Yu J, Han Y, Li Y, et al. (2017) Mechanism and kinetics of the reduction of hematite to magnetite with CO–CO<sub>2</sub> in a micro-fluidized bed. *Minerals* 7: 209. <https://doi.org/10.3390/min7110209>
43. Du W, Yang S, Pan F, et al. (2017) Hydrogen reduction of hematite ore fines to magnetite ore fines at low temperatures. *J Chem*. <https://doi.org/10.1155/2017/1919720>



AIMS Press

© 2023 the Author(s), licensee AIMS Press. This is an open access article distributed under the terms of the Creative Commons Attribution License (<http://creativecommons.org/licenses/by/4.0>)